Original article

Nuclear Medicine Communications

Clinical usefulness of ^{99m}Tc-HYNIC-TOC, ^{99m}Tc(V)-DMSA, and ^{99m}Tc-MIBI SPECT in the evaluation of pituitary adenomas

Vladimir R. Vukomanovic[a], Milovan Matovic[a], Mirjana Doknic[f], Vesna Ignjatovic[a], Ivana Simic Vukomanovic[b], Svetlana Djukic[c], Miodrag Peulic[d] and Aleksandar Djukic[e]

Background **The aim of this study was to evaluate the behavioral uptake and ability to diagnose pituitary adenoma (PA) using tumor-seeking radiopharmaceuticals, and to provide a semiquantitative analysis of tracer uptake in the pituitary region.**

Patients and methods **The study included 33 (13 hormonally active and 20 nonfunctioning) patients with PA and 45 control participants without pituitary involvement. All patients ($n = 78$) underwent single photon emission computed tomography (SPECT) imaging with technetium-99m-labeled hydrazinonicotinyl-tyr^3-octreotide (^{99m}Tc-HYNIC-TOC), dimercaptosuccinic acid (^{99m}Tc(V)-DMSA) and hexakis-2-methoxyisobutylisonitrile (^{99m}Tc-MIBI). A semiquantitative analysis of abnormal uptake was carried out by drawing identical regions of interest over the pituitary area and the normal brain on one transverse section that shows the lesion most clearly. The pituitary uptake to normal brain uptake (P/B) ratio was calculated in all cases.**

Results **The result of this study confirms that the SPECT semiquantitative method, with all three tracers, showed statistically significant differences between the PA group and the controls. However, ^{99m}Tc-HYNIC-TOC scintigraphy could have the highest diagnostic yield because of the smallest overlap between the P/B ratios between adenoma versus nonadenoma participants (the receiver operating characteristic curve P/B ratio cut-off value was 13.08). In addition, only ^{99m}Tc-MIBI SPECT have the diagnostic potential to detect secreting PAs, with statistically significant differences between groups ($P < 0.001$), with an receiver operating characteristic curve P/B ratio cut-off value of 16.72.**

Conclusion **A semiquantitative analysis of increased focal tracer uptake in the sellar area showed that ^{99m}Tc-HYNIC-TOC is a highly sensitive and reliable tumor-seeking agent for detecting PA, whereas ^{99m}Tc-MIBI SPECT is a highly sensitive and specific method in differentiating hormone-secreting pituitary tumor.** ***Nucl Med Commun*** **40:41–51**

Nuclear Medicine Communications 2019, **40**:41–51

Keywords: **^{99m}Tc(V)-DMSA, ^{99m}Tc-HYNIC-TOC, ^{99m}Tc-MIBI, pituitary adenoma, single photon emission computed tomography**

Departments of [a]Nuclear Medicine, [b]Social Medicine, [c]Internal Medicine, [d]Surgery, [e]Pathophysiology, Faculty of Medical Sciences, University of Kragujevac, Kragujevac and [f]Department of Internal Medicine, Faculty of Medicine, University of Belgrade, Belgrade, Serbia

Correspondence to Vladimir R. Vukomanovic, MD, PhD, Clinical Center Kragujevac, Centre for Nuclear medicine and Molecular Imaging, 30 Zmaj Jovina Street, 34000 Kragujevac, Serbia
Tel: +381 6339 2991; fax: +381 3450 5388; e-mail: vukomanovic@gmail.com

Received 2 September 2018 **Accepted** 2 October 2018

Introduction

Early diagnosis of pituitary tumors is of paramount importance for treatment and prognostic purposes. The differential diagnosis of pituitary adenomas (PA), which account for 90% of sellar and parsellar lesions, is generally made on the basis of clinical, endocrinological, and radiological characteristics [1–3]. Hormonally active PAs present different challenges and evaluation can be geared toward the specific hypersecretory syndrome [1,4,5]. Microadenomas (< 10 mm in size) are usually the cause of endocrine dysfunction, whereas PAs larger than 10 mm in diameter, are more likely to be nonfunctioning pituitary adenoma (NFPA) and may have a clinically aggressive course and present with pituitary hypofunction, neurological deficits, invasion into the parasellar compartment, and sphenoid sinuses [3,4,6]. In the diagnostic work-up, MRI plays a principal role in defining the localization and tumor size [2,7,8]. However, even with the use of modern imaging techniques, the differential diagnosis of NFPAs, recurrent/residual tumor, and scar/necrotic tissue after surgery may still be difficult in some cases [9–11]. In addition, the differentiation between secreting and nonsecreting adenomas is not possible using classical MRI [7].

Molecular imaging in nuclear medicine may potentially enable further characterization of these tumors, at the molecular and cellular level, using various tumor-seeking radiopharmaceuticals (tracers) [7,12,13]. The somatostatin receptor scintigraphy (SRS) identifies intracranial tumors on the basis of the presence of positive receptors for somatostatin (SSTR) [14–16]. SSTRs are expressed by both normal

DOI: 10.1097/MNM.0000000000000931

pituitary glands and pituitary tumors, and have been found in most cases of all secreting PAs [16–19]. For other variants, such as nonfunctioning adenomas, controversial results have been reported [10,20,21]. Although considerable literature exists on ^{111}In-labeled peptides in PA imaging [22–27], the use of technetium-99m-labeled EDDA-hydrazinonicotinyl-tyr^3-octreotide (^{99m}Tc-HYNIC-TOC) has increased at a considerable pace in recent years, owing to the similar pharmacokinetic profile and better imaging characteristics [28–31].

Technetium-99m-hexakis-2-methoxyisobutylisonitrile (^{99m}Tc-MIBI) is a well-known tumor imaging agent, whose uptake and retention within tumor cells are related to perfusion and the number of mitochondria, reflecting cell viability. Therefore, cells with high metabolic activity can show high ^{99m}Tc-MIBI uptake [32, 33]. Although it has been considered a potential tumor imaging agent for detecting brain tumors [34,35], only a few studies have reported the accumulation of ^{99m}Tc-MIBI in pituitary tumors [36–39], indicating a strong affinity for PAs.

Dimercaptosuccinic acid with pentavalent ^{99m}Tc under alkaline conditions ^{99m}Tc(V)-DMSA, gains its role in the prognosis and diagnosis of malignant tumors [40]. Approximately 95% of benign and malignant primary brain tumors are detected by ^{99m}Tc(V)-DMSA single photon emission computed tomography (SPECT) scans, such as low-grade or high-grade gliomas, meningiomas, and schwannomas [40–42]. Several reports suggest that ^{99m}Tc (V)-DMSA uptake by PAs is related to proliferative activity, which is either directly related to tumor grade or to the mitotic activity [43–45].

As many studies have reported the accumulation of all three tracers within the normal pituitary gland, the aim of this study was to assess the utility of these tumor-seeking radiopharmaceuticals in the evaluation of PAs. Accordingly, we carried out a semiquantitative SPECT analysis for the detection of adenomatous lesions, as well as the clinical significance of this imaging method.

Patients and methods

Study population

This cross-sectional study was carried out during the year 2015–2017 in the Clinical Center Kragujevac, Serbia. The research was carried out in accordance with the Declaration of Helsinki of the World Medical Association and was approved by the institutional ethical committee. Informed consent was obtained from all of the study participants.

The study involved 78 (60 women, 18 men) consecutive patients, older than 18 years of age, of whom 33 had PAs (mean age 47.78 ± 12.78, range: 24–69 years). The control group included 45 patients with adrenal tumors (mean age 54.60 ± 11.48, range: 31–72 years) and without pituitary involvement.

All patients and controls underwent pituitary MRI using the same protocol. To achieve a final diagnosis, clinical, biochemical, and hormonal parameters, as well as immunopathological findings after transsphenoidal surgery were included. All PAs in this study included NFPA ($n = 20$), prolactin (PRL)-secreting ($n = 8$), growth hormone (GH)-secreting ($n = 3$), and adrenocorticotropic hormone (ACTH)-secreting ($n = 2$).

Twenty-one patients underwent surgery in Clinical center Belgrade, Serbia (two PRL-secreting, three GH-secreting, two ACTH-secreting, and 14 NFPA), and the pathological report confirmed the presence of PA; the remaining six patients with PRL-secreting adenomas received medical treatment or stereotactic radiosurgery. Preoperative MRI examinations were performed in all of these patients. The remaining six patients with clinically nonfunctioning microadenoma were scheduled for regular follow-up examinations.

Exclusion criteria were defined in the protocol study. Therefore, some patients were excluded after randomization according to these protocols. Important exclusion criteria were as follows: pregnancy, breast feeding, diseases and administration of drugs influencing hormonal secretion, history of malignant disease, and other severe life-threatening diseases (pre-existing coronary and other atherosclerotic vascular disease). Other tumors and inflammatory diseases of the sellar region, disorders and diseases potentially affecting the pituitary glands, 'empty sella,' and cystic lesions were ruled out.

Determination of biochemical parameters

The following hypophyseal hormones were determined in all patients: GH, ACTH, PRL, thyroid stimulating hormone, follicle stimulating hormone, and luteinizing hormone. The determinations were performed immunoradiometrically (IRMA Cis-Biointernational, Gif-sur Yvette, France) and with radioimmunoassay (RIA Cis-Biointernational) measured on a Wallac Wizard 1470 Automatic gamma counter (PerkinElmer Life Sciences, Wallac Oy, Finland). Hormone inhibition and stimulation tests were carried out: inhibition tests with dexamethasone for ACTH-secreting tumors and oral glucose overload test for GH-secreting tumors. Serum progesterone, testosterone and β-estradiol, plasma free metanephrine and catecholamines, serum aldosterone and plasma renin activity, and insulin-like growth factor 1 were measured photometrically by Olympus AU 400 photometer, using kits of Olympus Life manufacturer and materials of Science Europa GmbH (Irish Branch), Lismeehen O' Callaghan's Mills, Co. Clare, Ireland.

Diagnostic imaging

Radiological imaging: all MRI pituitary studies were carried out on a 1.5-T closed magnet (Magnetom Symphony; Siemens, Germany). Imaging of pituitary region included T1-weighted and T2- weighted images, plus chemical shift imaging (in-phase and out-of-phase

imaging) and/or dynamic-gadolinium sequences. The chemical shift imaging signal loss on MRI was calculated quantitatively by measuring the signal intensity index. All MRI data were reviewed independently by a radiologist and a neurosurgeon.

In the imaging evaluation of adrenal glands, conventional morphological characteristics were assessed using a 64-row multidetector computed tomography scanner (Aquilion; Toshiba, Japan). The standard examination protocol comprises a precontrast computed tomography to provide density measurements of lesions. Two post-contrast scanning were performed after iodinated contrast agent injection started (wash-in at 60 s and wash-out at 15 min). The percentage of absolute or relative contrast enhancement were calculated for each adrenal mass.

Nuclear Medicine Imaging: all patients underwent radionuclide imaging with ^{99m}Tc-HYNIC-TOC, ^{99m}Tc (V)-DMSA, and ^{99m}Tc-MIBI within a 4–6-week period between each scan. All tracers were prepared using a commercially available kit with recommended administered activity according to the manufacturer's instructions.

Acquisition protocol: early (15 min after injection) and late (2 h after injection) whole-body scans were performed in the anterior and posterior projections (256×1024 matrix, 12 cm/min), on a dual-head Gamma camera (Syngo-E.cam; Siemens), equipped with low-energy high-resolution collimators, at a window setting of 140 keV. A SPECT scan of the brain was performed in the same manner with the following parameters: 360° noncircular orbit (body contour mode) step and shoot mode, at 30 s per view, 1.23 zoom. The acquired data were collected in a 128×128 image matrix, and reconstructed using an iterative ordered subset expectation algorithm. Transverse, coronal, and sagittal projections were reconstructed.

The analysis of SPECT images was both qualitative and semiquantitative.

All images were first evaluated qualitatively (visually) by two experienced nuclear medicine physicians. The readers were blinded to all clinical information. The visual appearance of a focal uptake of the tracer localized in the sellar area, greater than background activity, was considered a positive finding (Fig. 1).

A subsequent semiquantitative analysis was carried out of all findings to compare the tumor uptake of radiopharmaceutical with nontumor tissue. All data were analyzed on a Syngo-E.cam system using a region-of-interest (ROI) technique for the semiquantitative analysis of major organ and tumor uptake. For this purpose, pituitary-to-normal brain ratios (P/B) were calculated after constructing the ROI around the pituitary area and the normal brain on one transverse section that showed the pituitary area most clearly. The mean ROI values (total counts/total pixels) were measured and the P/B ratios were obtained in all patients. The background ROI of the brain was drawn above the sella turcica not attached to the choroid plexus (Fig. 2).

Statistical analysis

All statistical analyses were carried out using SPSS for Windows 20.0 (SPSS Inc., Chicago, Illinois, USA). Continuous variables are summed as arithmetic means, medians, and SD, and categorical variables as proportions (percentages of categories). The estimates of sensitivity, specificity, positive and negative predictive values, and accuracy were obtained from qualitative analysis using 2×2 contingency tables. For the statistical semiquantitative analysis, the T/NT ratios were expressed as medians and mean ± SD. Paired *t*-tests, Mann–Whitney test, analysis of variance, and Wilcoxon tests were used to determine statistically significant differences in the semiquantitative analyses of the groups, as appropriate. For all statistical tests that were used, *P* value of less than 0.05 value was considered to be statistically significant.

Results

The diagnosis of PAs was made by MRI, hormonal analysis, and/or by histopathological evaluation in all surgical cases. All control patients had a negative pituitary MRI.

Of the 33 PAs, 25 were microadenomas and eight were macroadenomas (three with parasellar extension). The mean diameter of the microadenomas was 6.61 ± 2.08 (range: 3–10 mm) and that of the macroadenomas was 13.42 ± 2.38 (range: 11–39 mm).

All eight macroadenomas had positive MRI findings. With histology as the gold standard, this imaging modality failed to detect small (< 5 mm in diameter) PAs in seven (28%) of 25 microadenomas, whereas all these cases were scintigraphy positive using ^{99m}Tc-HYNIC-TOC (Table 1).

For all patients in whom PA was ultimately confirmed to be present and the adrenal controls, both readers independently interpreted the scintigraphic images. There was no interreader disagreement. The image findings were than compared with the standard clinical and imaging criteria or/and the final histopathologic diagnosis of the removed tumors after transsphenoidal surgery. On the basis of qualitative (visually) analysis, we assessed the number of true-positive (TP), true-negative (TN), false-positive (FP), and false-negative (FN) findings. Sensitivity was calculated according to the formula TP/(TP + FN), specificity TN/(TN + FP), positive predictive value according to TP/(TP + FP), negative predictive value according to TN/(TN + FN), and accuracy according to (TP + TN)/(TP + TN + FP + FN). The distribution of findings in the different groups of patients is shown in Table 2.

In the present study, scintigraphy with ^{99m}Tc-HYNIC-TOC showed uptake in 30 out of 33 patients with

Fig. 1

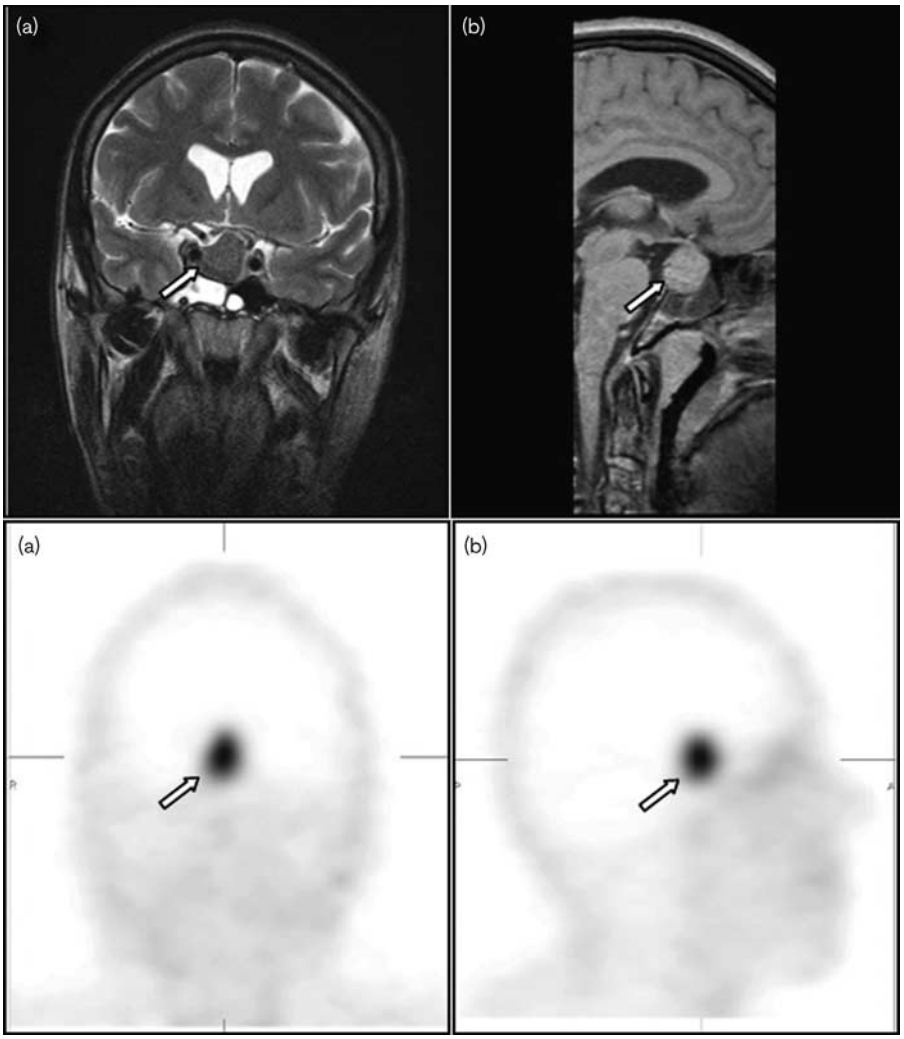

Sagittal T2W-postcontrast (a) and coronal T1W-postcontrast (b) MRI in patients with pituitary adenoma (arrow). ^{99m}Tc-HYNIC-TOC SPECT sagittal (a) and coronal (b) images at the same patient: focal somatostatin-avid tracer uptake is the sellar area (arrow) with a P/B ratio of 31.3 confirming the diagnosis of an adenoma. P/B, pituitary uptake to normal brain uptake; SPECT, single photon emission computed tomography; ^{99m}Tc-HYNIC-TOC, technetium-99m-labeled EDDA-hydrazinonicotinyl-tyr^3-octreotide.

confirmed PA (all three negative were nonfunctioning microadenomas), with an overall sensitivity of 90.91%, and in eight out of 37 patients without pituitary involvement, with an overall specificity of 82.22%.

Furthermore, the tumor uptake ratios on studies with all three radiopharmaceuticals were compared with each other using a semiquantitative analysis.

In SPECT studies, the P/B ratios were significantly higher in the PA group compared with the controls with ^{99m}Tc-HYNIC-TOC ($P<0.001$), with ^{99m}Tc(V)-DMSA ($P<0.001$), and with ^{99m}Tc-MIBI ($P=0.001$; Fig. 3). However, there was a difference between the P/B ratios among the groups. The highest was with ^{99m}Tc-HYNIC-TOC 22.02±5.61 (median 21.93, range: 14.85–35.85) compared with the control group, 8.19±4.43 (median 7.01, range: 2.07–17.89), with ^{99m}Tc(V)-DMSA 16.55±5.76 (median 14.56, range: 6.13–26.87) compared with the control group 6.39±3.44 (median 6.52, range: 1.44–13.52), and ^{99m}Tc-MIBI 19.66±10.47 (median 18.06, range: 7.71–46.63) compared with the control group 8.81±4.69 (median 11.23, range: 2.33–15.45). The smallest overlap was between the P/B ratios in the control group and the pathological group with ^{99m}Tc-HYNIC-TOC scintigraphy.

Qualitative analysis of scintigraphic images in terms of PA's functionality is presented in Table 3. According to these results, only ^{99m}Tc-MIBI scintigraphy showed high diagnostic potential in detecting secreting forms of these tumors, whereas the other two tracers showed lower sensitivity, specificity, as well as accuracy. For the

Fig. 2

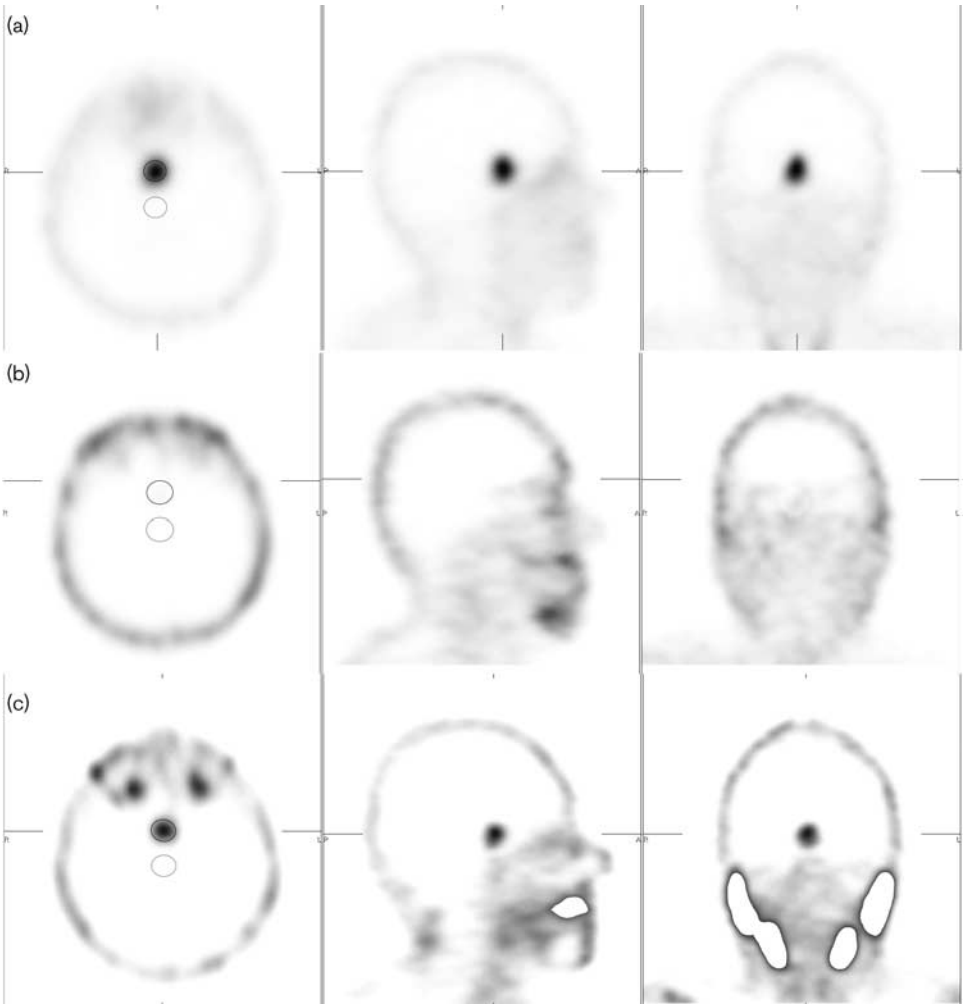

Transverse, sagittal, and coronal slices of the acquired SPECT, postprocessing using the iterative reconstruction (OSEM) method using ^{99m}Tc-HYNIC-TOC (a), ^{99m}Tc(V)-DMSA (b), and ^{99m}Tc-MIBI (c) in the same patient. An ROI was drawn on the transversal image around the tumor, whereas a mirror ROI was drawn above the sella turcica not attached to the choroid plexus. ROI, region-of-interest; SPECT, single photon emission computed tomography; ^{99m}Tc-HYNIC-TOC, technetium-99m-labeled EDDA-hydrazinonicotinyl-tyr^3-octreotide; ^{99m}Tc-MIBI, technetium-99m-hexakis-2-methoxyisobutylisonitrile.

Table 1 Discordant result of MRI and pathology reports of pituitary masses

Patient no.	Age	Sex	Size (mm)[a]	Histopathology diagnosis	MRI	^{99m}Tc-HYNIC-TOC (P/B ratio)
1	32	Female	28	Pituitary adenoma	Negative	Positive (19.02)
2	63	Female	35	Pituitary adenoma	Negative	Positive (22.63)
3	54	Female	36	Pituitary adenoma	Negative	Positive (25.54)
4	65	Female	38	Pituitary adenoma	Hypodense structure	Positive (24.12)
5	59	Male	40	Pituitary adenoma	Empty sella	Positive (29.54)
6	53	Female	45	Pituitary adenoma	Hypodense structure	Positive (32.18)
7	57	Male	55	Pituitary adenoma	Hypodense structure	Positive (34.58)

P/B, pituitary uptake to normal brain uptake; ^{99m}Tc-HYNIC-TOC, technetium-99m-labeled EDDA-hydrazinonicotinyl-tyr3-octreotide.
[a]The largest diameters of pituitary lesions.

subsequent semiquantitative scoring of tracer uptake, the difference between the P/B ratios in patients with ^{99m}Tc-MIBI scintigraphy, across the three groups, was statistically significant ($P < 0.001$). The higher P/B ratio was found in the secreting adenomas group, 32.36 ± 8.80 (median 33.46, range: 20.23–46.63), than in those with

Table 2 The qualitative single photon emission computed tomography analysis in characterization of pituitary tumors

				Predictive value (95% CI) (%)	
$n=78$	Sensitivity (95% CI) (%)	Specificity (95% CI) (%)	Accuracy (95% CI) (%)	Positive	Negative
^{99m}Tc-HYNIC-TOC	90.91 (75.67–98.08)	82.22 (67.95–92.00)	85.90 (76.17–92.74)	78.95 (66.47–87.65)	92.50 (80.61–97.34)
^{99m}Tc(V)-DMSA	81.82 (64.54–91.03)	77.78 (62.91–88.80)	79.49 (68.84–87.80)	72.97 (60.43–82.68)	85.37 (73.56–92.44)
^{99m}Tc-MIBI	78.79 (61.09–91.02)	75.56 (60.46–87.12)	76.92 (66.00–85.71)	70.27 (57.86–80.27)	82.93 (71.14–90.54)

CI, confidence interval; ^{99m}Tc-HYNIC-TOC, technetium-99m-labeled EDDA-hydrazinonicotinyl-tyr^3-octreotide; ^{99m}Tc-MIBI, technetium-99m-hexakis-2-methoxyisobutylisonitrile.

Fig. 3

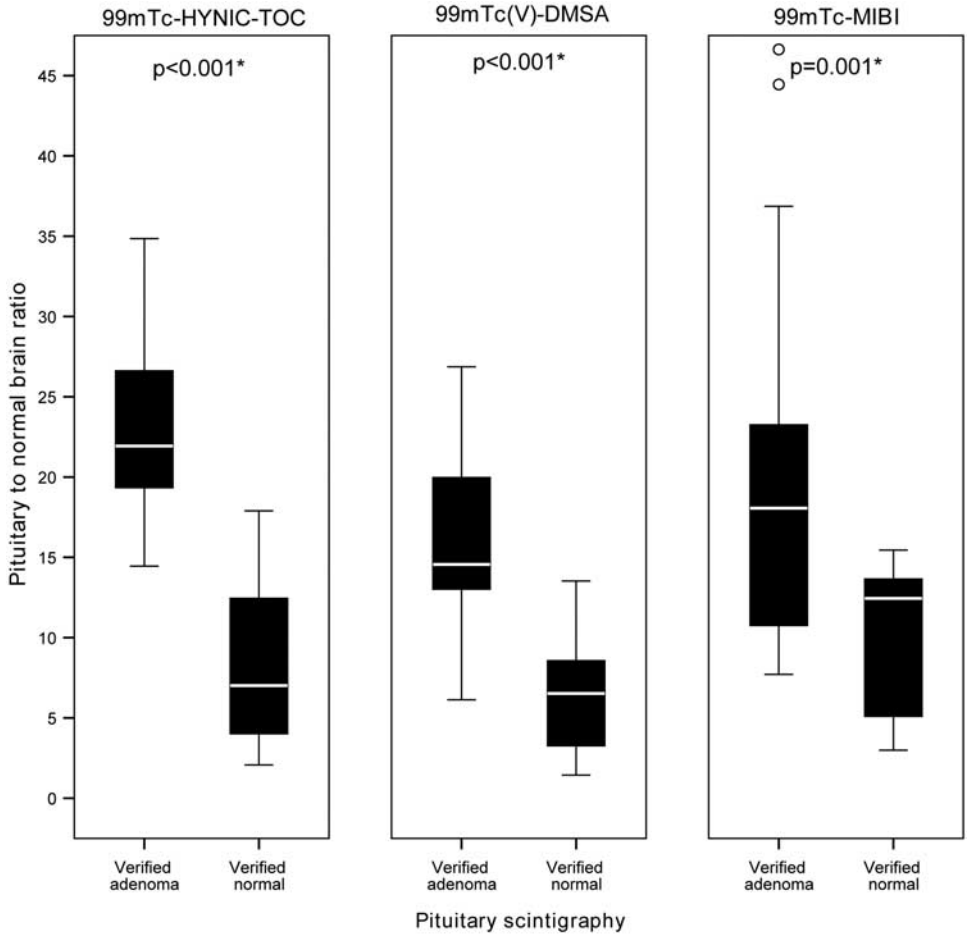

Distribution of P/B ratios in the three studied groups showing a statistically significant difference (Mann–Whitney *U*-test) between pituitary adenomas ($n=33$) and the control group ($n=45$). P/B, pituitary uptake to normal brain uptake.

Table 3 Qualitative single photon emission computed tomography analysis in the characterization of pituitary adenoma function

				Predictive value (95% CI) (%)	
$n=33$	Sensitivity (95% CI) (%)	Specificity (95% CI) (%)	Accuracy (95% CI) (%)	Positive	Negative
^{99m}Tc-MIBI	84.62 (54.55–98.08)	85.00 (62.11–96.79)	84.85 (68.10–94.89)	78.57 (55.74–91.44)	89.47 (70.10–96.86)
^{99m}Tc(V)-DMSA	61.54 (31.58–86.14)	55.00 (31.53–76.94)	57.58 (39.22–74.52)	47.06 (31.75–62.95)	68.75 (49.87–82.95)
^{99m}Tc-HYNIC-TOC	53.58 (25.13–80.78)	35.00 (15.39–59.22)	42.42 (25.48–60.78)	35.00 (22.86–49.46)	53.58 (33.55–72.94)

CI, confidence interval; ^{99m}Tc-HYNIC-TOC, technetium-99m-labeled EDDA-hydrazinonicotinyl-tyr^3-octreotide; ^{99m}Tc-MIBI, technetium-99m-hexakis-2-methoxyisobutylisonitrile.

Fig. 4

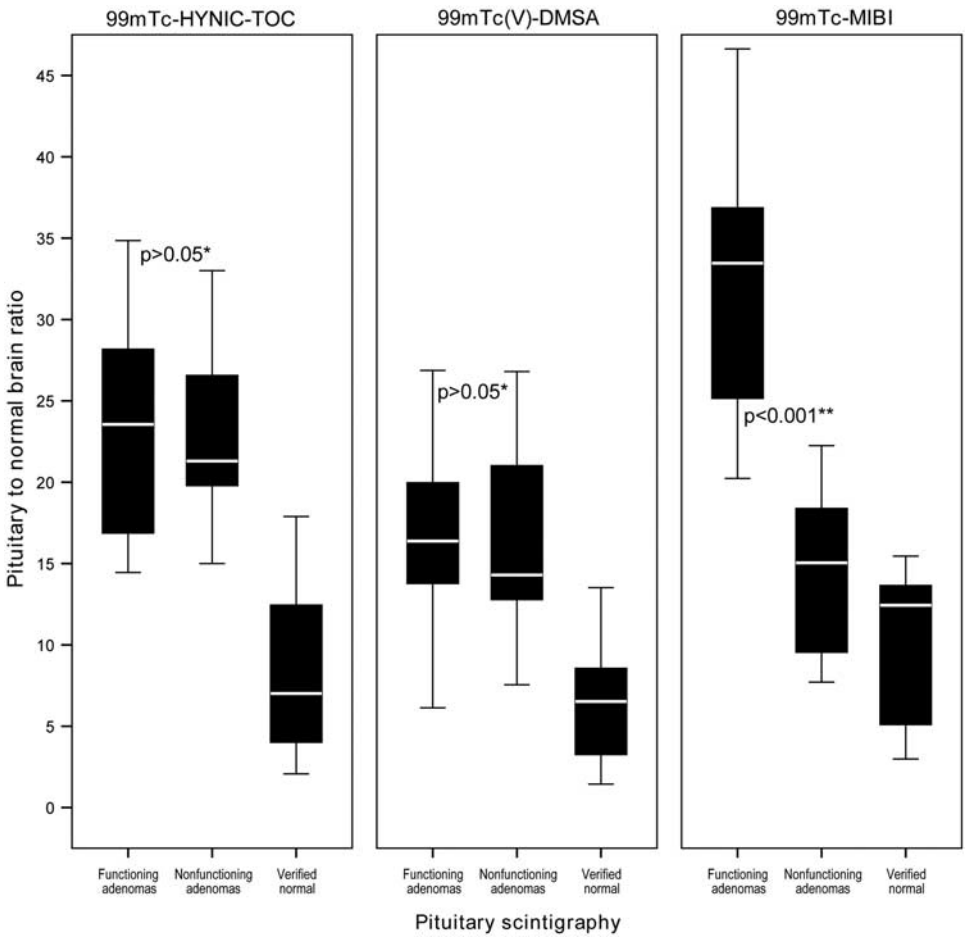

Distribution of P/B ratios in the three studied groups revealing statistically significant difference (ANOVA, post-hoc analysis) only with ^{99m}Tc-MIBI SPECT between functioning ($n = 13$) and nonfunctioning pituitary adenomas ($n = 20$). ANOVA, analysis of variance; P/B, pituitary uptake to normal brain uptake; ^{99m}Tc-MIBI, technetium-99m-hexakis-2-methoxyisobutylisonitrile.

nonsecreting forms, 14.15 ± 4.77 (median 15.04, range: 7.71–22.25), and this was statistically significant in the post-hoc analysis ($P < 0.001$; Fig. 4).

The accuracy of the P/B score in classifying correctly the existence of PA and functional activity was evaluated using the receiver operating characteristic (ROC) analysis. The ROC curves analysis showed that ^{99m}Tc-HYNIC-TOC scintigraphy provided the best discriminating power in detecting PA at the optimal P/B ratio cut-off value of 13.08 (area = 0.902, $P < 0.001$, sensitivity 82%, specificity 84%) (Fig. 5). Analysis of the ROC curves showed that the ^{99m}Tc-MIBI P/B ratio of 16.72 is the best cut-off value for distinguishing secreting from nonsecreting PAs (area = 0.851, $P < 0.001$, sensitivity 70%, specificity 86%; Fig. 6).

Discussion

One of the greatest challenges of modern neuroendocrinology is to differentiate between the mass found in the sellar area from other clinically insignificant changes [1,2]. Although PAs are the most common cause of a sellar mass, there are a number of neoplastic, inflammatory infectious, and vascular abnormalities that should be considered by the clinicians. Therefore, a comprehensive clinical assessment and long-term follow-up are necessary [1,2,7].

The development of various imaging modalities has resulted in the diagnosis of previously unsuspected PAs (incidentalomas) [7,46,47]. Specific clinical approaches and recommendations suggest that pituitary MRI is the preferred diagnostic imaging modality for the evaluation of sellar and parasellar tumors [7,8,11]. The majority of NFPA either secrete inadequate amounts of hormones or inactive hormonal fragments; thus, the differential diagnosis is currently made on the basis of radiological characteristics [3,11,12]. It is sometimes difficult, however, to differentiate the lesion because of the small size, such as corticotrope adenomas, with FN results of 45–62% [48], as well as the MRI technique used and variability in observer experience [49].

Fig. 5

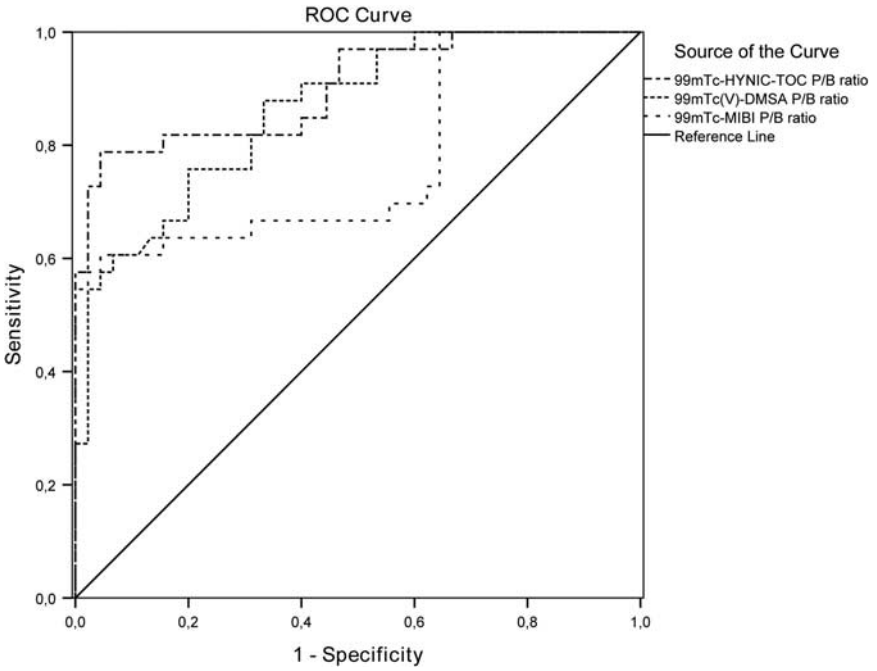

Summary ROC curves of diagnostic accuracy of ^{99m}Tc-HYNIC-TOC, ^{99m}Tc(V)-DMSA, and ^{99m}Tc-MIBI SPECT for distinguishing pituitary adenoma from nonadenomas. ROC, receiver operating characteristic; ^{99m}Tc-HYNIC-TOC, technetium-99m-labeled EDDA-hydrazinonicotinyl-tyr^3-octreotide; ^{99m}Tc-MIBI, technetium-99m-hexakis-2-methoxyisobutylisonitrile.

Fig. 6

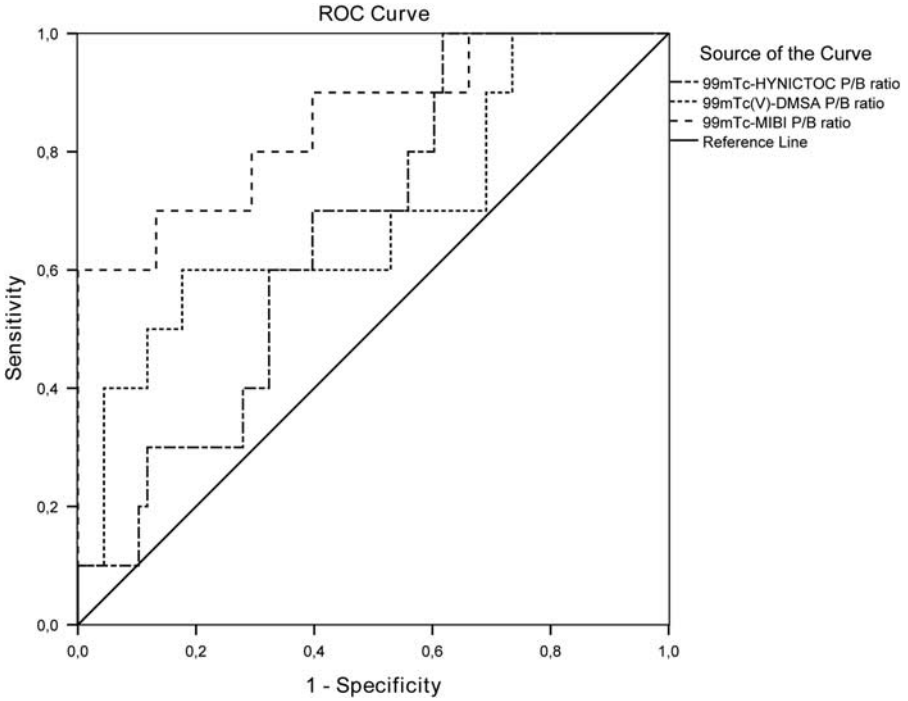

Summary ROC curves of diagnostic accuracy of ^{99m}Tc-HYNIC-TOC, ^{99m}Tc(V)-DMSA, and ^{99m}Tc-MIBI SPECT for distinguishing functioning from nonfunctioning pituitary adenomas. ROC, receiver operating characteristic; SPECT, single photon emission computed tomography; ^{99m}Tc-HYNIC-TOC, technetium-99m-labeled EDDA-hydrazinonicotinyl-tyr^3-octreotide; ^{99m}Tc-MIBI, technetium-99m-hexakis-2-methoxyisobutylisonitrile.

However, SPECT modality performed by a large field of view gamma camera enables the cross-sectional imaging of the pituitary region of the brain. An abnormal tracer accumulation in the sellar region could be considered a pathological finding [35,39,43]. In our study, we detected seven (28%) of 25 microadenomas using ^{99m}Tc-HYNIC-TOC SPECT, which were MRI negative. Four of these seven were hormonally active PAs.

Although many scintigraphic studies of brain tumors have been reported, there are only a few studies on PAs [36,37, 44,45].

The role of SRS in the diagnosis and differential diagnosis of PA is that it enables the visualization of tumors on the basis of the fundamental characteristics of membrane receptors [21–23]. This study results showed that ^{99m}Tc-HYNIC-TOC can significantly demonstrate high-grade visual uptake in PA compared with uptake within the normal pituitary gland, with a sensitivity of 90.91% (Table 1). Reports on the sensitivity of this technique have been variable, ranging from 36 to 90% [29,30,46]. Subsequently, the widespread use of [^{111}In]DTPA-Octreotide, whose pharmacokinetic is similar to ^{99m}Tc-HYNIC-TOC, showed that the sensitivity of SPECT technique ranged from 40 to 79% [22,25–27].

The diagnostic potential of qualitative scintigraphy with ^{99m}Tc(V)-DMSA and ^{99m}Tc-MIBI was slightly lower (Table 1), with overall sensitivities of 81.82 and 78.79%, respectively.

Consistent with these findings are the results of a few studies indicating that the ^{99m}Tc(V)-DMSA scintigraphy showed an overall sensitivity ranging from 71 to 95% in detecting PAs [43–45]. Furthermore, ^{99m}Tc-MIBI was found to have a strong affinity for PA, but not the normal pituitary gland [36,37]. Kunishio *et al.* [38] suggest that ^{99m}Tc-MIBI SPECT may be a useful technique for the diagnosis of PA, with an overall sensitivity of 85%. Accumulation of these tracers is generally related to the affinity for the tissue or lesions, not the size of the lesion [36,37,43–45,] which was also the case in our study.

Although several previous reports have shown increased uptake of ^{99m}Tc-HYNIC-TOC, ^{99m}Tc(V)-DMSA, and ^{99m}Tc-MIBI in the PAs, only a few articles have published results using a semiquantitative method. Our study methodology suggests a simple semiquantitative index to diagnose underlying pituitary abnormalities.

In our series, the evaluation of pituitary involvement showed that the mean P/B ratios between the PA group and the controls with ^{99m}Tc-HYNIC-TOC on SPECT studies were higher than ^{99m}Tc(V)-DMSA and ^{99m}Tc-MIBI (Fig. 3).

^{99m}Tc-HYNIC-TOC P/B uptake ratios obtained our research (median 21.93, range: 14.85–35.85) are higher to results reported from other studies [23,27,31]. The semiquantitative analysis using ^{99m}Tc(V)-DMSA and ^{99m}Tc-MIBI is consistent with the findings of similar studies [37,44].

To date, this is the first study to evaluate PA function using a semiquantitative scintigraphic method with all three tracers. Despite the apparent major benefit of the use of scintigraphy with all three tracers, we emphasize that the ^{99m}Tc-HYNIC-TOC semiquantitative method could have the highest diagnostic yield because of the smallest overlap between the P/B ratios between adenoma versus nonadenoma patients. Moreover, the presence of high-affinity SSTRs in most PA implies that the ^{99m}Tc-HYNIC-TOC may be useful for predicting the response to somatostatin analogue treatment and for the postsurgical detection of small or residual tumors that are undetectable on MRI [23,24]. In addition, SRS is not only useful in the diagnosis and follow-up but also in the radionuclide therapy of pituitary tumors [47–49].

In terms of the likelihood of the detection of secreting PAs, the qualitative analysis of ^{99m}Tc-MIBI scintigraphy showed the highest sensitivity (84.62%), specificity (85.00%) as well as accuracy (84.85%) (Table 2).

The overall sensitivity of ^{99m}Tc(V)-DMSA and ^{99m}Tc-HYNIC-TOC, by the qualitative scintigraphic analysis described, was significantly lower, and is consistent with previous studies that concluded that scintigraphy with these tracers was not sufficiently sensitive for the evaluation of patients with secreting PAs [44,50].

All analyses carried out in this study suggested that only ^{99m}Tc-MIBI scintigraphy has the diagnostic potential to detect secreting PAs, with a statistically significant difference ($P < 0.001$) between groups (Fig. 4). The explanation for this phenomenon is based upon knowledge of higher ^{99m}Tc-MIBI uptake and distribution in cells with high mitochondrial activity [33,34]. Thus, ^{99m}Tc-MIBI scintigraphy provides information of a functional nature directly related to tumor pathophysiology [3–5].

The main limitation of this study was the inability to generate a three-dimensional ROI conforming to the geometrical shapes of an adenoma. This parameter would have been a better reflection of the actual tumor volume, and hence a better uptake index could have been calculated. Nevertheless, this study provides a valid technique to calculate the P/B ratio taking into account the largest cross-sectional area of each individual slice. This method yields consistent results with a small SD. Another limitation is that the study population was relatively small, and our results need to be confirmed in larger clinical studies.

Conclusion

Our preliminary result indicates that the semiquantitative SPECT method should therefore be used in the diagnosis of PAs. The important advantages of a computer-assisted semiquantitative approach to scintigraphic

analysis are that it provides standardized image formation and objective evaluation criteria, which significantly improves both the sensitivity and the specificity in detecting PAs. Despite the poorer resolution of the gamma camera, high adenoma tracer uptake was sufficient to enable SPECT detection.

Although the administration of three tracers provides considerably more information, it is not convenient in everyday clinical practice. To investigate the existence of PA, ^{99m}Tc-HYNIC-TOC was shown to be a promising imaging agent. Furthermore, ^{99m}Tc-MIBI offers the highest diagnostic accuracy for distinguishing secreting from nonsecreting forms of these tumors.

Our findings are relevant to the differential diagnosis of PAs, clarify conflicting data in previous reports of tumor-seeking tracers, and may have clinical implications for the noninvasive identification of affected individuals.

Acknowledgements

Conflicts of interest

There are no conflicts of interest.

References

1 Molitch ME. Diagnosis and treatment of pituitary adenomas: a review. *JAMA* 2017; **317**:516–524.
2 Syro LV, Rotondo F, Ramirez A, Di Ieva A, Sav MA, Restrepo LM, *et al*. Progress in the diagnosis and classification of pituitary adenomas. *Front Endocrinol* 2015; **6**:97.
3 Lake MG, Krook LS, Cruz SV. (2013) Pituitary adenomas: an overview. *Am Fam Physician* 2013; **88**:319–327.
4 Melmed S. Pituitary tumors. *Endocrinol Metab Clin North Am* 2015; **44**:1–9.
5 Melmed S. Pituitary medicine from discovery to patient-focused outcomes. *J Clin Endocrinol Metab* 2016; **101**:769–777.
6 Chatzellis E, Alexandraki KI, Androulakis II, Kaltsas G. Aggressive pituitary tumors. *Neuroendocrinology* 2015; **101**:87–104.
7 Chaudhary V, Bano S. Imaging of the pituitary: recent advances. *Indian J Endocrinol Metab* 2011; **15**:S216–S223.
8 Famini P, Maya MM, Melmed S. Pituitary magnetic resonance imaging for sellar and parasellar masses: ten-year experience in 2598 patients. *J Clin Endocrinol Metab* 2011; **96**:1633–1641.
9 Fenstermaker R, Abad A. Imaging of pituitary and parasellar disorders. *Continuum (Minneap Minn)* 2016; **22**:1574–1594.
10 Sharma P, Mukherjee A, Bal C, Malhotra A, Kumar R. Somatostatin receptor-based PET/CT of intracranial tumors: a potential area of application for 68Ga-DOTA peptides? *Am J Roentgenol* 2013; **201**:1340–1347.
11 Smith KA, Leever JD, Chamoun RB. Prediction of consistency of pituitary adenomas by magnetic resonance imaging. *J Neurol Surg B Skull Base* 2015; **76**:340–343.
12 De Herder WW. Molecular imaging of pituitary pathology. *Front Horm Res* 2016; **45**:133–141.
13 De Herder WW, Reijs AE, Feelders RA, van Aken MO, Krenning EP, van der Lely AJ, *et al*. Diagnostic imaging of dopamine receptors in pituitary adenomas. *Eur J Endocrinol* 2007; **156**:S53–S56.
14 De Herder WW, Kwekkeboom DJ, Feelders RA, van Aken MO, Lamberts SW, van der Lely AJ, *et al*. Somatostatin receptor imaging for neuroendocrine tumors. *Pituitary* 2006; **9**:243–248.
15 Feelders RA, de Herder WW, Neggers SJ, van der Lely AJ, Hofland LJ. Pasireotide, a multi-somatostatin receptor ligand with potential efficacy for treatment of pituitary and neuroendocrine tumors. *Drugs Today (Barc)* 2013; **49**:89–103.
16 Ben-Shlomo A, Melmed S. Pituitary somatostatin receptor signaling. *Trends Endocrinol Metab* 2010; **21**:123–133.
17 Thodou E, Kontogeorgos G, Theodossiou D, Pateraki M. Mapping of somatostatin receptor types in GH or/and PRL producing pituitary adenomas. *J Clin Pathol* 2006; **59**:274–279.
18 Van der Hoek J, Waaijers M, van Koetsveld PM, Sprij-Mooij D, Feelders RA, Schmid HA, *et al*. Distinct functional properties of native somatostatin receptor subtype 5 compared with subtype 2 in the regulation of ACTH release by corticotroph tumor cells. *Am J Physiol Endocrinol Metab* 2005; **289**:E278–E287.
19 Jaquet P, Ouafik L, Saveanu A, Gunz G, Fina F, Dufour H, *et al*. Quantitative and functional expression of somatostatin receptor subtypes in human prolactinomas. *J Clin Endocrinol Metab* 1999; **84**:3268–3276.
20 Ramírez C, Cheng S, Vargas G, Asa SL, Ezzat S, Gonzalez B, *et al*. Expression of Ki-67, PTTG1, FGFR4, and SSTR 2, 3, and 5 in nonfunctioning pituitary adenomas: a high throughput TMA, immunohistochemical study. *J Clin Endocrinol Metab* 2012; **97**:1745–1751.
21 Faglia G, Bazzoni N, Spada A, Arosio M, Ambrosi B, Spinelli F, *et al*. In vivo detection of smatostatin receptors in patients with functionless pituitary adenomas by means of a radioiodinated analog of somatostatin ([123I] SDZ 204-090). *J Clin Endocrinol Metab* 1991; **73**:850–856.
22 Acosta-Gomez MJ, Muros MA, Llamas-Elvira JM, Ramirez A, Ortega S, Sabatel G, *et al*. The role of somatostatin receptor scintigraphy in patients with pituitary adenoma or postsurgical recurrent tumors. *Br J Radiol* 2005; **78**:110–115.
23 Duet M, Ajzenberg C, Benelhadj S, Lajeunie E. Somatostatin receptor scintigraphy in pituitary adenomas: a somatostatin receptor density index can predict hormonal and tumoral efficacy of octreotide in vivo. *J Nucl Med* 1999; **40**:1252–1256.
24 Maecke HR, Reubi JC. Somatostatin receptors as targets for nuclear medicine imaging and radionuclide treatment. *J Nucl Med* 2011; **52**:841–844.
25 Lauriero F, Pierangeli E, Rubini G, Resta M, D'Addabbo A. Pituitary adenomas: the role of 111In-DTPA-octreotide SPET in the detection of minimal post-surgical residues. *Nucl Med Commun* 1998; **19**:1127–1134.
26 Rieger A, Rainov NG, Elfrich C, Klaua M, Meyer H, Lautenschläger C, *et al*. Somatostatin receptor scintigraphy in patients with pituitary adenoma. *Neurosurg Rev* 1997; **20**:7–12.
27 Colao A, Lastoria S, Ferone D, Varrella P, Marzullo P, Pivonello R, *et al*. The pituitary uptake of 111In-DTPA-DPhe1-octreotide in the normal pituitary and in pituitary adenomas. *J Endocrinol Invest* 1999; **22**:176–178.
28 Gabriel M, Decristoforo C, Donnemiller E, Ulmer H, Rychlinski CW, Mather SJ, *et al*. An intrapatient comparison of ^{99m}Tc-EDDA/HYNIC-TOC with 111In-DTPA-octreotide for diagnosis of somatostatin receptor-expressing tumors. *J Nucl Med* 2003; **44**:708–716.
29 Li F, Chen LB, Jing HL, Du YR, Chen F. Preliminary clinical application of 99mTc-HYNIC-TOC imaging in somatostatin receptor-positive tumors. *Zhongguo Yi Xue Ke Xue Yuan Xue Bao* 2003; **25**:563–566.
30 Płachcińska A, Mikołajczak R, Maecke HR, Młodkowska E, Kunert-Radek J, Michalski A, *et al*. Clinical usefulness of ^{99m}Tc-EDDA/HYNIC-TOC scintigraphy in oncological diagnostics: a preliminary communication. *Eur J Nucl Med Mol Imaging* 2003; **30**:1402–1406.
31 Oppizzi G, Cozzi R, Dallabonzana D, Orlandi R, Benini Z, Petroncini M, *et al*. Scintigraphic imaging of pituitary adenomas: an in vivo evaluation of somatostatin receptors. *J Endocrinol Invest* 1998; **21**:512–519.
32 Moretti JL, Hauet N, Caglar M, Rebillard O, Burak Z. To use MIBI or not to use MIBI? That is the question when assessing tumour cells. *Eur J Nucl Med Mol Imaging* 2005; **32**:836–842.
33 Hindié E, Ugur Ö, Fuster D, ODoherty M, Grassetto G, Ureña P, *et al*. 2009 EANM parathyroid guidelines. *Eur J Nucl Med Mol Imaging* 2009; **36**:1201–1216.
34 Cecchin D, Chondrogiannis S, Della Puppa A, Rotilio A, Zustovich F, Manara R, *et al*. Presurgical ^{99m}Tc-sestamibi brain SPET/CT versus SPET: a comparison with MRI and histological data in 33 patients with brain tumours. *Nucl Med Commun* 2009; **30**:660–668.
35 Kunishio K, Morisaki K, Matsumoto Y, Nagao S, Nishiyama Y. Technetium-99m sestamibi single photon emission computed tomography findings correlated with P-glycoprotein expression, encoded by the multidrug resistance gene-1 messenger ribonucleic acid, in intracranial meningiomas. *Neurol Med Chir* 2003; **43**:573–580.
36 Kojima T, Mizumura S, Kumita SI, Kumazaki T, Teramoto A. Is technetium-99m-MIBI taken up by the normal pituitary gland? A comparison of normal pituitary glands and pituitary adenomas. *Ann Nucl Med* 2001; **15**:321–327.
37 Tiktinsky E, Horne T, Friger M, Agranovich S, Lantsberg S. Pituitary incidentalomas detected with technetium-99m MIBI in patients with suspected parathyroid adenoma: preliminary results. *World J Nucl Med* 2012; **11**:3–6.
38 Kunishio K, Okada M, Matsumoto Y, Nagao S, Nishiyama Y. Technetium-^{99m} sestamibi single photon emission computed tomography findings correlated with P-glycoprotein expression in pituitary adenoma. *J Med Invest* 2006; **53**:285–291.
39 Vukomanovic V, Matovic M, Doknic M, Ignjatovic V, Vukomanovic IS, Djukic S, *et al*. Adrenocorticotropin-producing pituitary adenoma detected with

^{99m}Tc-hexakis-2-methoxy-isobutyl-isonitrile single photon emission computed tomography. A case report. *Acta Endocrinol (Buc)* 2015; **11**:253–256.
40 Shukla J, Mittal BR. Dimercaptosuccinic acid: a multifunctional cost effective agent for imaging and therapy. *Indian J Nucl Med* 2015; **30**:295–301.
41 Tsiouris S, Pirmettis I, Chatzipanagiotou T, Ptohis N, Papantoniou V. Pentavalent technetium-^{99m} dimercaptosuccinic acid [^{99m} Tc-(V)DMSA] brain scintitomography – a plausible non-invasive depicter of glioblastoma proliferation and therapy response. *J Neurooncol* 2007; **85**:291–295.
42 Hirano T, Otake H, Shibasaki T, Tamura M, Endo K. Differentiating histologic malignancy of primary brain tumors: pentavalent technetium-99m-DMSA. *J Nucl Med* 1997; **38**:20–26.
43 Yamamura K, Suzuki S, Yamamoto I. Differentiation of pituitary adenomas from other sellar and parasellar tumors by ^{99m}Tc (V)-DMSA scintigraphy. *Neurol Med Chir* 2003; **43**:181–186.
44 Suzuki S, Yamamura K, Chang CC, Kojima Y, Yamamoto I, Ikegami T. ^{99m}Tc (V)-DMSA. A useful radio isotopic material for the diagnosis of pituitary adenoma. *CI Kenkyu* 2000; **22**:85–91.
45 Lastoria S, Colao A, Vergara E, Ferone D, Varrella P, Merola B, *et al.* Technetium-99m pentavalent dimercaptosuccinic acid imaging in patients with pituitary adenomas. *Eur J Endocrinol* 1995; **133**:38–47.
46 Artiko V, Afgan A, Petrović J, Radović B, Petrović N, Vlajković M, *et al.* Evaluation of neuroendocrine tumors with ^{99m}Tc-EDDA/HYNIC TOC. *Nucl Med Rev Cent East Eur* 2016; **19**:99–103.
47 Baldari S, Ferrau F, Alafaci C, Herberg A, Granata F, Militano V, *et al.* First demonstration of the effectiveness of peptide receptor radionuclide therapy (PRRT) with 111In-DTPA-octreotide in a giant PRL-secreting pituitary adenoma resistant to conventional treatment. *Pituitary* 2012; **15**:57–60.
48 Maclean J, Aldridge M, Bomanji J, Short S, Fersht N. Peptide receptor radionuclide therapy for aggressive atypical pituitary adenoma/carcinoma: variable clinical response in preliminary evaluation. *Pituitary* 2014; **17**:530–538.
49 Komor J, Reubi JC, Christ ER. Peptide receptor radionuclide therapy in a patient with disabling non-functioning pituitary adenoma. *Pituitary* 2014; **17**:227–231.
50 Colao A, Ferone D, Lombardi G, Lastoria S. (^{99m}) Technetium pentavalent dimercaptosuccinic acid scintigraphy in the follow-up of clinically nonfunctioning pituitary adenomas after radiotherapy. *Clin Endocrinol (Oxf)* 2002; **56**:713–721.